[CANCER RESEARCH 55, 4240–4242, October 1, 1995]

Advances in Brief

Radiation-induced Apoptosis of Ewing's Sarcoma Cells: DNA Fragmentation and Proteolysis of Poly(ADP-ribose) Polymerase[1]

Viatcheslav A. Soldatenkov,[2] Sarada Prasad, Vicente Notario, and Anatoly Dritschilo

Department of Radiation Medicine, Division of Radiation Research, Georgetown University Medical Center, Washington, DC 20007

Abstract

Ewing's sarcoma (ES) cells express high levels of poly(ADP-ribose) polymerase (PADPRP) and are responsive to killing by ionizing radiation. We have determined that ionizing radiation induced a pronounced but reversible G_2-M phase cell cycle arrest that was maximum by 24 h after exposure. Following the release from this block, floating cells began to appear. These floating cells were shown to be apoptotic by flow cytometric and DNA fragmentation analyses. We found that apoptosis is a significant component of radiation-induced death in ES cells and that this is accomplished in conjunction with proteolytic cleavage of PADPRP. Two fragments of M_r 25,000 and M_r 29,000 containing the PADPRP DNA-binding domain were identified in floating (apoptotic) cells, whereas only the full-length M_r 116,000 native protein was detected in adherent cells that retained DNA intact. These data are consistent with PADPRP cleavage being an early step in the apoptotic cascade of biochemical events in ES cells after ionizing radiation exposure.

Introduction

ES[3] is a bone tumor of childhood that is characterized by the presence of poorly differentiated round cells that are believed to be of neuroectodermal origin (1). Treatment of ES patients generally includes a combined modality approach with radiation therapy and chemotherapy (2). Clinically, the tumors are responsive to such treatment; however, the overall cure rate is poor due to frequent presentation with metastatic disease (3, 4). We have reported previously that ES cells express elevated levels of PADPRP (EC 2.4.2.30), an enzyme which catalyzes the transfer of the ADP-ribose moiety from NAD to nuclear proteins (5). Furthermore, treatment of cells with the PADPRP inhibitor 3-aminobenzamide resulted in sensitization of ES cells to killing by ionizing radiation (6). We have attributed the observed radiation sensitivity of ES cells to overexpression and enhanced PADPRP activity in response to DNA damage, although the underlying mechanism remains to be elucidated.

Exposure of cells to lethal doses of DNA-damaging agents, including ionizing radiation, results in their necrotic or apoptotic death (7, 8). It has been demonstrated recently that proteolytic cleavage of PADPRP into fragments of M_r 25,000 and M_r 85,000 is an early marker of chemotherapy-induced apoptosis (9). Cleavage of PADPRP to a M_r 85,000 fragment has also been found to be a characteristic feature of both Fas- and tumor necrosis factor-induced apoptosis of mammalian cells (10). Therefore, we asked whether apoptosis is a significant component of radiation-induced death in ES cells and whether the specific proteolysis of PADPRP is an integral component of the radiation-induced cell death pathway. The data presented in this report show that ionizing radiation-induced apoptosis of ES cells is accompanied by the proteolytic cleavage of PADPRP.

Materials and Methods

Cells and Culture Conditions. The ES cell line A4573 was kindly provided by Dr. Timothy Kinsella of the University of Wisconsin Medical School (Madison, WI). Cells were cultured in Eagle's minimal essential medium (GIBCO) supplemented with 10% fetal bovine serum, 1% L-glutamine, 100 units/ml penicillin, and 100 μg/ml streptomycin at 37°C in an atmosphere of 5% CO_2 in air.

Irradiation. All irradiations were performed at room temperature, in air, using a ^{137}Cs source in a "JL Shepard MARK I" laboratory irradiator at a dose rate of 2.37 Gy/min.

FACS Analysis. Cells ($1–2 \times 10^6$) harvested at various times after irradiation were washed with PBS and then vortexed gently while 95% ethanol was added slowly to a final concentration of 80%. The fixed cells were stored at −20°C. Prior to analysis by FACS, cells were centrifuged, washed with PBS once, and incubated at 37°C for 30 min, followed by staining with propidium iodide (50 μg/ml) in PBS. The cell cycle phase distribution was determined using a FACS Star Plus flow cytometer (Becton Dickinson FACS System) and "ModFit" DNA distribution modeling software. Results were presented as the number of cells relative to the amount of DNA as indicated by the intensity of fluorescence. The percentage of hypodiploid (apoptotic) cells, which appeared in the cell cycle distribution as cells with DNA content less than G_1, was assessed simultaneously with cell cycle analysis.

DNA Gel Electrophoresis. To assess DNA integrity, total cellular DNA was prepared as described previously (11). Adherent and floating cells were harvested separately 72 h after irradiation, washed in PBS, and resuspended in lysis buffer [10 mM Tris-HCl (pH 8.0), 5 mM EDTA, 1% SDS, and 50 μg/ml RNase A), followed by incubation for 1 h at 37°C. Cell lysates were treated with proteinase K (100 μg/ml) in the presence of 1 M NaCl for 3 h at 37°C. DNA was extracted with phenol:chloroform:isoamyl alcohol, precipitated with ethanol, recovered by centrifugation, and resuspended in TE-buffer [10 mM Tris-HCl (pH 7.5) and 1 mM EDTA). DNA preparations were end-labeled with Klenow and [α-^{32}P]dCTP as described (12). Unincorporated nucleotides were removed by three consecutive precipitation cycles with ethanol. Recovered DNA samples were applied onto 2% agarose gels and electrophoresed for 16 h at 1.5 V/cm. Gels were dried at 50°C and exposed to X-ray film.

Western Analysis. Total cellular proteins (50 μg/sample) from control or irradiated cells were resolved on SDS-10% polyacrylamide gels and transferred to Immobilon (Millipore) membranes. PADPRP immunodetection was performed as described previously using a rabbit polyclonal antiserum raised against a synthetic peptide encompassing the first 20 NH_2-terminal amino acids of the human PADPRP (13). Equal sample loading was confirmed by reprobing the same blots with a rabbit polyclonal antiserum against glyceraldehyde-3-phosphate dehydrogenase (Trevigen).

Results and Discussion

The cell cycle distribution of ES cells was determined by flow cytometry at various times after irradiation. As depicted in Fig. 1*A*, ionizing radiation caused a pronounced accumulation of cells in G_2-M phases, with a concomitant decrease of the percentages of cells in G_1 and S phases. The fraction of cells in the G_2-M phase increased to 55% of the total population by 24 h after radiation exposure. The

Received 7/6/95; accepted 8/18/95.

The costs of publication of this article were defrayed in part by the payment of page charges. This article must therefore be hereby marked *advertisement* in accordance with 18 U.S.C. Section 1734 solely to indicate this fact.

[1] This work was supported by Grant CA 58986 from the NIH.

[2] To whom requests for reprints should be addressed, at Department of Radiation Medicine, Georgetown University Medical Center, The Research Building, E-207, 3970 Reservoir Road, Washington, DC 20007.

[3] The abbreviations used are: ES, Ewing's sarcoma; PADPRP, poly(ADP-ribose) polymerase; FACS, fluorescence-activated cell sorting.

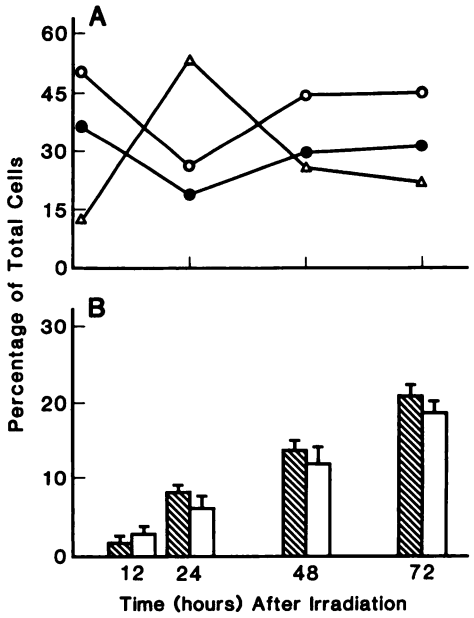

Fig. 1. Response of ES cells to irradiation at 7 Gy: G_2-M delay and apoptosis onset. *A*, radiation-induced G_2-M delay. The percentage of cells in the G_1 (○), S (●), and G_2-M (△) phases at various time intervals after irradiation was determined by FACS. *B*, accumulation of floating cells coincides with the appearance of apoptotic cells after irradiation. Floating cells (▨) were collected and scored after irradiation at the time points indicated. The percentage of apoptotic cells (□) was determined by FACS analysis as described in "Materials and Methods." *Points*, the means of duplicate experiments; *bars*, SE.

DNA fragmentation and laddering upon electrophoresis is frequently associated with apoptotic process (7, 8, 11, 12). To confirm that apoptosis was actually ongoing in irradiated ES cells, DNA fragmentation analyses were carried out in both adherent and floating cells (Fig. 3*a*). Agarose gel electrophoresis of DNA isolated from

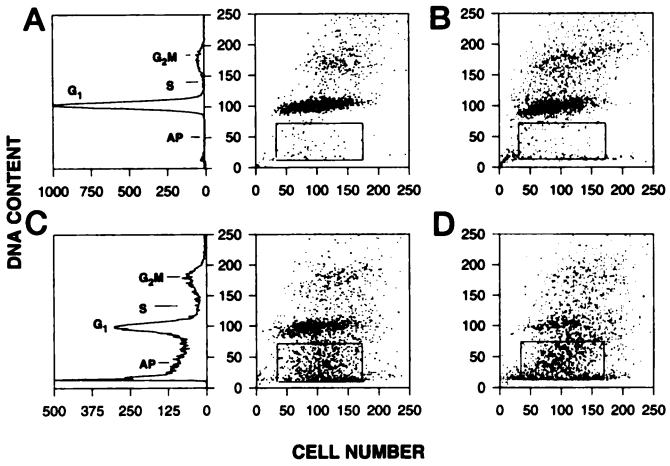

Fig. 2. Appearance of hypodiploid (apoptotic) cells in irradiated (7 Gy) ES cells. The positions of cells with fractional DNA content (*AP*) are indicated below G_1 on DNA histograms on the *left*. Dot-plots of FACS analysis data (*A-D*) on the *right* represent frequency distribution of DNA in the hypodiploid (apoptotic) and diploid (viable) cells. *Boxed areas* on the dot-plots, hypodiploid cells. *A*, unirradiated control cells; *C*, 72 h after irradiation of cells; *D*, floating population of cells represented in *C*; *B*, adherent cells of *C*.

postirradiation G_2-M delay appeared to be reversible in ES cells, and 72 h after irradiation, the G_2-M phase cell fraction approached the baseline levels. It has been proposed that radiation-induced G_2 arrest allows repair of DNA damage to prevent its fixation prior to entering mitosis (14). Cells that sustain substantial genomic damage have been hypothesized to be eliminated by the induction of a cell death cascade. Dying cells are shed into the culture medium, allowing the extent of cell death to be assessed as an increase in the number of detached (floating) cells (15). Our data on the quantitative representation of the population of floating cells as a function of time after irradiation is in agreement with this hypothesis. Fig. 1*B* shows that following the release from G_2-M arrest floating cells began to appear and reached approximately 20% of the total population by 72 h after irradiation. Flow cytometric analysis allows unequivocal assessment of the numbers of hypodiploid (apoptotic) cells and cells with diploid DNA content (nonapoptotic) following induction of the cell death by chemical compounds or irradiation (16). When we determined the number of hypodiploid cells as function of time, the appearance and time-dependent increase of the population of apoptotic (hypodiploid) cells coincided with the accumulation of floating cells after irradiation (Fig. 1*B*).

Fig. 2 represents the dot-plots of the quantitative DNA analyses in irradiated ES cells. The DNA histograms on the *left* show that the cells with fractional DNA content map below the cells in G_1, and these regions were considered to represent the population of apoptotic cells. Fig. 2*A* shows the relative distribution of cells with haploid and diploid DNA contents in logarithmically growing ES cells. The numbers of hypodiploid cells in the total population of irradiated cells (Fig. 2*C*) are significantly higher compared to those in control, unirradiated cells (Fig. 2*A*). At the same time, when adherent (Fig. 2*B*) and floating (Fig. 2*D*) populations of irradiated cells were analyzed independently, approximately 60% of floating cells were found to be apoptotic, while only 5% of the cells remaining attached after irradiation had a fractional DNA content.

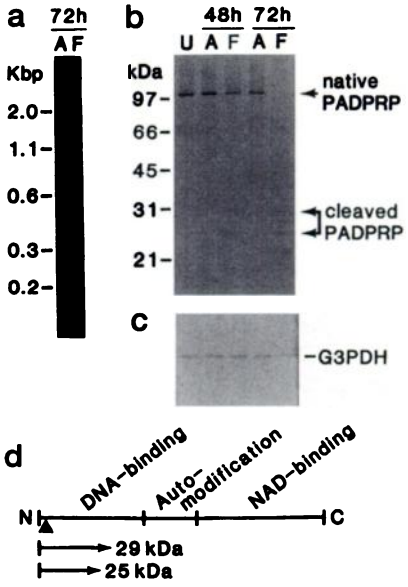

Fig. 3. DNA fragmentation and specific cleavage of PADPRP in apoptotic ES cells. Adherent (*A*) and floating (*F*) cells were collected separately 48 or 72 h after irradiation at 7 Gy. Control, unirradiated cultures (*U*) contained less than 3% of floating cells and were analyzed in bulk. *a*, agarose gel electrophoresis of DNA. A typical "ladder" pattern indicates an internucleosomal DNA fragmentation in floating cells after irradiation. No DNA fragmentation was detected in control, unirradiated cells (data not shown). The migration of molecular size markers (kilobase pairs) is indicated. *b*, immunodetection of PADPRP in ES cells after irradiation. Total cellular proteins (50 μg) were resolved by SDS-10% PAGE, transferred to Immobilon-P membranes, and subjected to Western blotting with polyclonal antiserum raised against a synthetic peptide encompassing the 20 NH_2-terminal amino acids of human PADPRP. *Arrowheads* on the *right*, native M_r 116,000 protein and cleavage products of PADPRP recognized by the anti-PADPRP probe. *Left*, molecular size markers. *c*, Western blot analysis of the cell lysates used in *b* with antibody to glyceraldehyde-3-phosphate dehydrogenase for protein loading equivalence. *d*, schematic representation of the functional domains of PADPRP. The location of the epitopes recognized by the anti-PADPRP antiserum is indicated by *triangle* at the NH_2-terminal end. The fragments of the DNA-binding domain, which appeared in apoptotic cells, are indicated with *arrows* at the *bottom*.

floating cells 72 h after irradiation demonstrated a ladder-like pattern; the degraded DNA was present in oligomers that were multiples of approximately 180–200 bp, suggesting internucleosomal cleavage. At the same time, adherent cells retained their high molecular weight DNA intact. This is consistent with the view that loss of viability leads to cell detachment and that accumulation of floating cells may be considered as an indicator of ongoing cell death.

We next analyzed the apoptosis-associated proteolysis of PADPRP in irradiated ES cells. The products of PADPRP cleavage were detected in floating cells (Fig. 3*b*) over the same time interval as hypodiploid (apoptotic) cells appeared (Fig. 1*B*). Using an antiserum against NH_2-terminal end of DNA-binding domain of PADPRP, we detected M_r 25,000 and M_r 29,000 protein fragments. In the adherent cells, at 48 h after irradiation the M_r 116,000 native PADPRP was intact, whereas in the floating cells, there was a decrease in the intensity of the native enzyme giving rise to the cleavage products. It was also evident that by 72 h after irradiation, in the floating cell population the M_r 116,000 PADPRP had undergone complete proteolysis. This process appeared to be closely associated with ongoing cell death because no PADPRP degradation was detected in cells remaining attached (Fig. 3*b*). Based on the intactness of glyceraldehyde-3-phosphate dehydrogenase (Fig. 3*c*), probed with specific antibody under identical conditions, radiation-induced cleavage of PADPRP seemed to be specific and not related to protein turnover. These data provide support for a potential role of PADPRP proteolysis in radiation-induced apoptosis of ES cells.

Recently, the specific proteolytic cleavage of PADPRP to fragments consisting of a M_r 25,000 DNA-binding domain and a M_r 85,000 fragment containing mainly its automodification and NAD-binding domains have been detected in human leukemia and breast cancer cells during chemotherapy-induced apoptosis (9). The M_r 85,000 fragment of PADPRP has been identified also during Fas- and tumor necrosis factor-induced apoptosis of mammalian cells (10). These data, taken together, imply that specific proteolytic cleavage of PADPRP may be an early event or perhaps a prerequisite for the onset of apoptotic cell death triggered by various effectors. Although the cleavage of PADPRP seems to be rather specific, the nature of the protease(s) responsible for this process remains to be established. A protease activity that shares certain features with the interleukin β-converting enzyme (prICE), which has been detected recently in extracts from cells committed to apoptosis (17). This protease has been implicated in the specific proteolysis of PADPRP into fragments of M_r 85,000 and M_r 25,000 in leukemic cells (9). In our case, the M_r 25,000 and M_r 29,000 fragments of the DNA-binding domain of PADPRP appeared in ES cells during radiation-induced apoptosis (Fig. 3). The M_r 29,000 fragment corresponded in size and location to the shortest NH_2-terminal polypeptide obtained by trypsin digestion of PADPRP (18). It should be noted that prICE activity was resistant to cysteine and serine protease inhibitors (17) and appeared to be different from trypsin-like proteases. Such data suggest that several proteolytic enzymes may be responsible for PADPRP cleavage, probably depending on tissue specificity and/or type of the effector triggering apoptosis. Several lines of evidence suggest that proteases act in a cascade of biochemical events resulting in programmed cell death (9, 10, 17, 19–21). However, the pathway(s) of their activation, their possible cross-interactions, the nature of target proteins, and whether these putative targets are intermediate or end points in the apoptotic pathway remain to be elucidated.

One of the possible implications of PADPRP cleavage in the apoptotic cascade results from the proposed "nick-protection" mechanism of polymerase action (22). According to this theory, auto-poly(ADP-ribosyl)ation of PADPRP effects its release from DNA strand breaks and allows access for DNA repair enzymes to the lesions (22). Radiation-induced proteolytic cleavage of PADPRP in cells committed to apoptosis may result in accumulation of DNA-binding PADPRP fragments (Fig. 3) and reduced catalytic activity of polymerase (9). Block of automodification prevents DNA-binding fragments from detaching from DNA and may result in fixation of DNA lesions. Such a mechanism may provide a basis for an additional "check point" to eliminate cells retaining substantial long-lived genomic damage by activation of the apoptotic cascade. Whether this possibility has functional significance remains to be established.

References

1. Lipinski, M., Hirsch, M. R., Deagostini-Bazin, H., Yamada, O., Tursz, T., and Goridis, C. Characterization of neural cell adhesion molecules (NCAM) expressed by Ewing and neuroblastoma cell lines. Int. J. Cancer, *40:* 81–86, 1987.
2. Kinsella, T. J., Mitchell, J. B., McPherson, S., Miser, J., Triche, T., and Glatstein, E. *In vitro* radiation studies on Ewing's sarcoma cell lines and human bone marrow: application to the clinical use of total body irradiation (TBI). Int. J. Radiat. Oncol. Biol. Phys., *10:* 1005–1011, 1984.
3. Brown, A. P., Fixsen, A. A., and Plowman, P. N. Local control of Ewing's sarcoma: an analysis of 67 patients. Br. J. Radiol., *60:* 261–268, 1987.
4. Weichselbaum, R. R., Beckett, M. A., Simon, M. A., McCaluley, C., Haraf, D., Awan, A., Samuels, B., Nachman, J., and Dritschilo, A. *In vitro* radiobiological parameters of human sarcoma cell lines. Int. J. Radiat. Oncol. Biol. Phys., *15:* 937–942, 1988.
5. Prasad, S. C., Thraves, P. J., Bhatia, K. G., Smulson, M. E., and Dritschilo, A. Enhanced poly (adenosine diphosphate ribose) polymerase activity and gene expression in Ewing's sarcoma cells. Cancer Res., *50:* 38–43, 1990.
6. Thraves, P., Mossman, K. L., Brennan, T., and Dritschilo, A. Differential sensitization of human tumor cells by 3-aminobenzamide and benzamide: inhibitors of poly(ADP-ribosylation). Int. J. Radiat. Biol., *50:* 961–972, 1986.
7. Wyllie, A. H., Kerr, J. F. R., and Currie, A. R. Cell death: the significance of apoptosis. Int. Rev. Cytol., *68:* 251–306, 1980.
8. Nakano, H., and Shinohara, K. X-ray-induced cell death: apoptosis and necrosis. Radiat. Res., *140:* 1–9, 1994.
9. Kaufman, S. H., Desnoyers, S., Ottaviano, Y., Davidson, N. E., and Poirier, G. G. Specific proteolytic cleavage of poly(ADP-ribose) polymerase: an early marker of chemotherapy-induced apoptosis. Cancer Res., *53:* 3976–3985, 1993.
10. Tewari, M., Quan, L. T., O'Rourke, K., Desnoyers, S., Zeng, Z., Beidler, D. R., Poirier, G. G., Salvesen, G. S., and Dixit, V. M. Yama/CPP32β, a mammalian homolog of CED-3, is a CrmA-inhibitable protease that cleaves the death substrate poly(ADP-ribose) polymerase. Cell, *81:* 801–809, 1995.
11. Soldatenkov, V. A., Denisenko, M. F., Khodarev, N. N., Votrin, I. I., and Filippovich, I. V. Early postirradiation chromatin degradation in thymocytes. Int. J. Radiat. Biol., *55:* 943–951, 1989.
12. Rösl, F. A simple and rapid method for detection of apoptosis in human cells. Nucleic Acids Res., *20:* 5243, 1992.
13. Prasad, S., Notario, V., and Dritschilo, A. Poly(ADP-ribose) polymerase in Hela cells: a high resolution two-dimensional gel analysis. Appl. Theor. Electrophoresis, *4:* 3–10, 1994.
14. McKenna, W. G., Iliakis, G., Weiss, M. C., Bernhard, E. J., and Muschel, R. J. Increased G_2 delay in radiation-resistant cells obtained by transformation of primary rat embryo cells with the oncogenes H-*ras* and v-*myc*. Radiat. Res., *125:* 283–287, 1991.
15. Shchepotin, I. B., Soldatenkov, V., Buras, R. R., Nauta, R. J., Shabahang, M., and Evans, S. R. T. Apoptosis of human primary and metastatic colon adenocarcinoma cell lines *in vitro* induced by 5-fluorouracil, verapamil, and hyperthermia. Anticancer Res., *14:* 1027–1032, 1994.
16. Gorczyca, W., Gong, J., Ardelt, B., Traganos, F., and Darzynkiewicz, Z. The cell cycle related differences in susceptibility of HL-60 to apoptosis induced by various antitumor agents. Cancer Res., *53:* 3186–3192, 1993.
17. Lazebnik, Y. A., Kaufmann, S. H., Desnoyers, S., Poirier, G. G., and Earshaw, W. C. Cleavage of poly(ADP-ribose) polymerase by a proteinase with properties like ICE. Nature (Lond.), *371:* 346–347, 1994.
18. Mazen, A., Menissier-de Murcia, J., Molinete, M., Simonin, F., Gradwohl, G., Poirier, G., and De Murcia, G. Poly(ADP-ribose) polymerase: a novel finger protein. Nucleic Acids Res., *17:* 4689–4698, 1989.
19. Soldatenkov, V. A., Denisenko, M. F., Alfyerova, T. M., and Filippovich, I. V. Chromatin degradation in thymus lymphocytes induced by radiation or dexamethasone: necessity of preliminary proteolysis. Radiobiologyia (Russ.), *31:* 180–187, 1991.
20. Shi, L., Kam, C-M., Powers, J. C., Aebersold, R., and Greenberg, A. H. Purification of three cytotoxic lymphocyte granule serine proteases that induce apoptosis through distinct substrate and target cell interactions. J. Exp. Med., *176:* 1521–1529, 1992.
21. Kumar, S. ICE-like proteases in apoptosis. Trends Biochem. Sci., *20:* 198–202, 1995.
22. Satoh, M. S., and Lindahl, T. Role of poly(ADP-ribose) formation in DNA repair. Nature (Lond.), *356:* 356–358, 1992.